BIOCHEMISTRY
including biophysical chemistry & molecular biology

Article

pubs.acs.org/biochemistry

Stabilization of an α/β-Hydrolase by Introducing Proline Residues: Salicylic Acid Binding Protein 2 from Tobacco

Jun Huang,[†,§,‡] Bryan J. Jones,[†,‡] and Romas J. Kazlauskas*[,†]

[†]Department of Biochemistry, Molecular Biology & Biophysics and The Biotechnology Institute, University of Minnesota, 1479 Gortner Avenue, Saint Paul, Minnesota 55108, United States

[§]School of Biological and Chemical Engineering, Zhejiang University of Science and Technology, Hangzhou 310023, People's Republic of China

Supporting Information

ABSTRACT: α/β-Hydrolases are important enzymes for biocatalysis, but their stability often limits their application. We investigated a plant esterase, salicylic acid binding protein 2 (SABP2), as a model α/β-hydrolase. SABP2 shows typical stability to urea (unfolding free energy 6.9 ± 1.5 kcal/mol) and to heat inactivation ($T_{1/2}^{15min}$ 49.2 ± 0.5 °C). Denaturation in urea occurs in two steps, but heat inactivation occurs in a single step. The first unfolding step in urea eliminates catalytic activity. Surprisingly, we found that the first unfolding likely corresponds to the unfolding of the larger catalytic domain. Replacing selected amino acid residues with proline stabilized SABP2. Proline restricts the flexibility of the unfolded protein, thereby shifting the equilibrium toward the folded conformation. Seven locations for proline substitution were chosen either by amino acid sequence alignment with a more stable homologue or by targeting flexible regions in SABP2. Introducing proline in the catalytic domain stabilized SABP2 to the first unfolding in urea for three of five cases: L46P (+0.2 M urea), S70P (+0.1), and E215P (+0.9). Introducing proline in the cap domain did not stabilize SABP2 (two of two cases), supporting the assignment that the first unfolding corresponds to the catalytic domain. Proline substitutions in both domains stabilized SABP2 to heat inactivation: L46P ($\Delta T_{1/2}^{15min}$ = +6.4 °C), S70P (+5.4), S115P (+1.8), S141P (+4.9), and E215P (+4.2). Combining substitutions did not further increase the stability to urea denaturation, but dramatically increased resistance to heat inactivation: L46P−S70P $\Delta T_{1/2}^{15min}$ = +25.7 °C. This straightforward proline substitution approach may also stabilize other α/β-hydrolases.

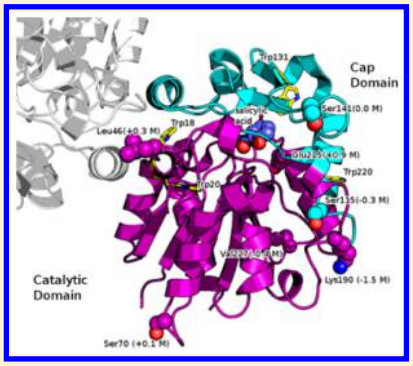

Most proteins are only marginally stable; that is, just stable enough for their natural function.[1,2] This marginal stability is not an inherent limitation of proteins since most proteins can be stabilized by single amino acid substitutions without compromising activity.[3] The reason for the marginal stability is that evolution cannot select for more than the minimum stability. Further, if a hyperstable protein arises randomly, further random amino acid substitutions are likely to decrease the stability of a protein until the stability drops to the minimum needed. The result is proteins that are just stable enough for their function.[4]

Most applications require stable enzymes that tolerate harsh reaction conditions or maintain activity for an extended time under moderate conditions.[5−7] Stable enzymes also tolerate numerous amino acid substitutions so are better starting points for protein engineering.[8−11] Because of the marginal stability of most proteins, most proteins for biocatalysis need to be stabilized. In this work, we use an esterase from tobacco, salicylic acid binding protein 2, as a model α/β-hydrolase fold protein. This protein superfamily contains many biocatalysts including esterases, lipases, hydroxynitrile lyases, and dehalogenases.[12−14] General methods to stabilize this class of enzymes would be broadly useful for biocatalysis. We analyze the unfolding of this model esterase and test proline substitution as a stabilization strategy.

Two common methods to measure protein stability are denaturant-induced unfolding and heat inactivation. Stable proteins adopt folded conformations in solution but are in equilibrium with a tiny fraction of unfolded protein conformations, Figure 1A. Adding denaturant, such as urea, disrupts hydrogen bonding between amide groups and shifts the equilibrium toward the unfolded form.[15−17] By measuring the equilibrium amount of unfolded protein in different concentrations of urea, one can extrapolate to the free energy of unfolding without urea.[18] Free energy values are particularly useful for rational, structure-based protein engineering since they relate directly to molecular properties like the contributions of flexibility to entropy.

Measuring the heat inactivation temperature of a protein also measures stability, Figure 1B. Heat shifts the equilibrium between folded and unfolded proteins by increasing the entropy contribution.[19] The unfolded state created by heating may differ from the unfolded state created by urea denaturation

Received: March 29, 2015
Revised: May 23, 2015
Published: June 25, 2015

DOI: 10.1021/acs.biochem.5b00333
Biochemistry 2015, 54, 4330−4341

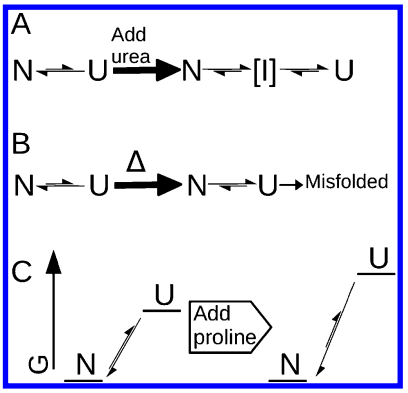

Figure 1. Simplified protein unfolding. (A) Native folded proteins (N) are in equilibrium with unfolded proteins (U); addition of denaturant such as urea shifts the equilibrium toward the unfolded form. Unfolding sometimes involves a stable, partially unfolded intermediate, [I]. (B) Heat also shifts the equilibrium toward the unfolded form; unfolded proteins can further aggregate or adopt misfolded conformations. (C) Replacement of an amino acid with proline can shift the folded–unfolded equilibrium toward the folded form. The proline should be placed in a location that does not disrupt the folded conformation. Proline limits the flexibility of the unfolded form reducing the entropic advantage of unfolding by ~1.2 kcal/mol.

because the destabilization mechanisms differ. In addition, heat denaturation usually irreversibly misfolds proteins, which prevents measuring the free energy of unfolding. Measuring stability by heat inactivation is easier than urea denaturation and more closely matches the goal of many applications, for the enzymes to remain active for long times at elevated temperatures.[20,21]

The α/β-hydrolase fold superfamily contains important enzymes for industrial applications.[22−24] For example, lipases, esterases, and hydroxynitrile lyases make enantiopure intermediates for pharmaceutical synthesis, and dehalogenases degrade pollutants. Stabilization of α/β-hydrolase fold enzymes is an important goal because it can extend the applications of these enzymes.

Most measurements of stability of α/β-hydrolases use heat-induced unfolding or deactivation. For example, lipase B from *Candida antarctica* unfolds at 46.4−54.8 °C,[21,25] Table 1. In a few cases, researchers measured the stability of α/β-hydrolases by urea-induced denaturation. For example, cutinase has an unfolding free energy of 7.7 ± 0.6 kcal/mol. The unfolding occurred in one step because cutinase contains only one domain.[26] For many α/β-hydrolases, the unfolding is more complex, and the free energy cannot be extracted from urea denaturation curves. Most α/β-hydrolases contain two domains: a cap, or lid, domain and a catalytic domain. If these domains unfold independently via a partly unfolded intermediate, then this more complex unfolding prevents extraction of free energies from the urea denaturation curves. For two special cases, esterases from thermophiles, the urea induced unfolding was a single cooperative transition and the free energies of unfolding could be derived from the data.[27,28]

Salicylic acid binding protein 2 from tobacco (SABP2) is a typical α/β-hydrolase.[33] This esterase catalyzes hydrolysis of methyl salicylate to salicylic acid as a plant defense signal. Like most α/β-hydrolases, SABP2 consists of two domains, Figure 2.

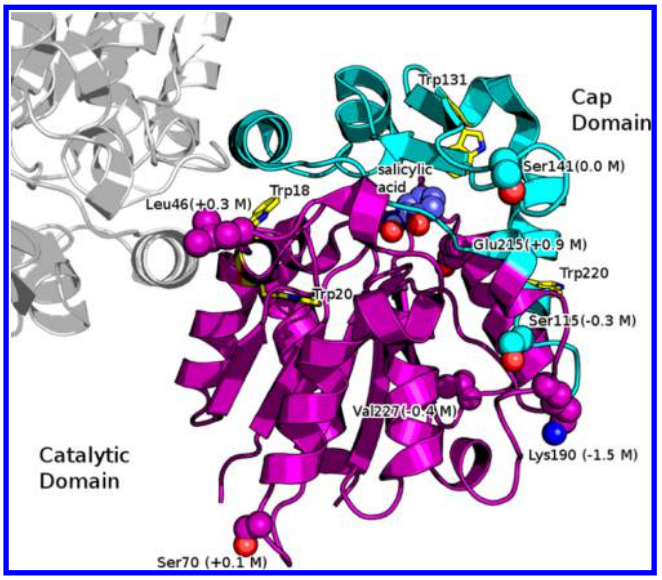

Figure 2. Ribbon representation of the structure of SABP2 (pdb entry 1y7i) showing the catalytic domain (magenta) and cap domain (turquoise) The active site lies at the interface of the two domains and contains bound product (salicylic acid, spheres, ocean-colored carbons). Exposure of the four tryptophan residues (yellow sticks) to solvent upon unfolding causes decreases in their fluorescence. The seven residues labeled and shown as spheres were substituted by proline. The changes in urea concentration needed to unfold the protein are marked, where positive values indicate stabilization. The second monomer (gray ribbons at the upper left) identifies location of the dimer interface.

The larger catalytic domain includes residues 1−111 and 185−262 (189 aa, 72% of the total in SABP2) and the smaller cap

Table 1. Stability of Selected α/β-Hydrolases Measured by Urea-Induced Denaturation and Heat-Induced Unfolding

enzyme	$C_{1/2}^{urea}$ [a] (M)	ΔG_{uw} [b] (kcal/mol)	T_m [c] (°C)	refs
lipase B from *Candida antarctica*	2.1[e]	*l*	46.4[g]−54.8[f,j]	21,25
acetyl esterase from *Escherichia coli*	6.2[f,g]	*l*	*l*	29
cutinase from *Fusarium solani pisi*	2.3[f]	7.7 ± 0.6	*l*	30
EST2 from *Alicyclobacillus acidocaldarius*	5.9[f,g]	15 ± 2	91[g,j]	27,28
AFEST from *Archeoglobus fulgidus*	7.1[f,g]	12 ± 2	99[g,j]	27,28
hydroxynitrile lyase from *Manihot esculenta*	*l*	*l*	~65[i]−69.3[g,j]	31,32
salicylic acid binding protein 2 (SABP2) from tobacco	2.3, 4.0[f]	3.5 ± 0.5 (1st transition), 3.4 ± 1.0 (2nd transition)[k]	49.0 ± 0.3[h]	this work

[a]Concentration of urea where the protein was half unfolded. [b]Free energy of unfolding in water extrapolated from the urea denaturation curves. When denaturation involved a partly unfolded intermediate, free energies could not be calculated. [c]Temperature where the protein is half unfolded. [e]Detected by activity assay. [f]Detected by fluorescence. [g]Detected by circular dichroism spectroscopy. [h]50% activity loss after 15 min incubation. [i]50% activity loss after 20 min incubation. [j]Measured by heating to increase temperature at a constant rate, typically 1 °C/min. [k]Free energies were calculated using a three state model. [l]Not reported.

DOI: 10.1021/acs.biochem.5b00333
Biochemistry 2015, 54, 4330−4341

domain includes residues 112−184 (73 aa, 28% of the total). The catalytic domain forms the α/β-hydrolase fold with a central core of β-sheets surrounded by α-helices. It contains the catalytic triad, the oxyanion hole for catalysis, and part of the substrate-binding site. The smaller cap (or lid) domain sits on top of the catalytic domain and forms the rest of the substrate-binding site. This cap domain contains a three-stranded antiparallel β-sheet and three helices. Each domain contains approximately equal numbers of polar and nonpolar amino acid residues. The catalytic domain contains 48% polar and 52% nonpolar, while the cap domain contains 51% polar and 49% nonpolar.

Substitution of amino acid residues with proline often increases protein stability.[34−36] The locations are chosen so the proline substitution does not affect the folded form. Proline restricts the flexibility of the unfolded protein compared with other amino acids, thus lowering the entropy gain upon unfolding by ∼4 cal/(deg mol) relative to alanine,[34] which corresponds to ∼1.2 kcal/mol at 300 K, Figure 1C. This change shifts the equilibrium toward the folded form, thereby stabilizing the protein.

In this work, we examine the unfolding of a typical α/β-hydrolase, salicylic acid binding protein 2 from tobacco (SABP2). We measured the stability of this esterase by both denaturant-induced unfolding and heat-induced inactivation. Urea-induced denaturation involved a partly unfolded intermediate and, thus, two unfolding transitions. Fitting the data to a three-state-model yielded free energies for each unfolding step. Introducing proline substitutions in the catalytic domain stabilized this protein to urea denaturation, while substitutions in either domain stabilized the protein to heat inactivation. The largest increase was a 25.7 °C increase in the heat inactivation temperature. A similar approach may also stabilize other α/β-hydrolase fold enzymes.

EXPERIMENTAL SECTION

General. Reagents were from Sigma-Aldrich unless otherwise noted. House deionized water was further purified with a Milli-Q water system (Millipore, Billerica, MA, USA, 18 MΩ purity). Integrated DNA Technologies (Coralville, IA) made the primers for the polymerase chain reaction and ACGT (Wheeling, IL) sequenced the DNA using BigDye terminator version 3.1. *Pfu* DNA polymerase was bought from Agilent Technologies (La Jolla, CA), *Dpn*I, DNA marker, and SDS-PAGE protein marker were from Invitrogen Life Technologies (Grand Island, NY). Isopropyl-β-D-thiogalactopyranoside (IPTG) was from Gold Biotechnology (St. Louis, MO) and ampicillin was bought from Roche Diagnostics. *Escherichia coli* DH5α and BL21 competent cells were prepared by calcium chloride treatment.[37] The protein concentrations were determined by the Bradford dye-binding assay at 595 nm using the Bio-Rad reagent and bovine serum albumin as the standard.[38] Protein gels were run on sodium dodecyl sulfate polyacrylamide gradient gels (NuPage 4−12% Bis-Tris gel from Invitrogen) using BenchMark protein ladder (5 μL/lane) as the standard. DNA gels were run using 0.8% ultrapure agarose with 1 × TAE buffer and 1 kb DNA ladder as a standard. Unless otherwise noted, *E. coli* strains for protein expression were grown in modified TB media (12 g/L bacto-tryptone, 24 g/L bacto-yeast extract, 9.86 g/L glucose with 2.3 g of KH_2PO_4 + 12.5 g of K_2HPO_4) containing 100 μg/mL ampicillin and incubated in unbaffled Erlenmeyer flasks at 37 °C shaking at 250 rpm. The amino acid sequences of *Me*HNL[39] and SABP2[33] were aligned using ClustalX 2.1.[40]

Site-Directed Mutagenesis of SABP2. The site-directed mutagenesis of salicylic acid binding protein 2 (SABP2) was carried out using the Stratagene QuikChange method where mutagenic primers, Table S1, Supporting Information, were used to amplify the entire plasmid using the polymerase chain reaction.[41] The reaction mixture contained DNA template (wild-type SABP2 gene with a C-terminal six-histidine tag in the pET21a(+) expression vector (pET21a(+)-SABP2), 1 ng), forward and reverse primers (100 μM, 1 μL of each), 10× PCR buffer (5 μL), dNTPs (0.9 μL 10 mM), *Pfu* DNA polymerase (1 μL, 2.5 U), and autoclaved water to a final volume of 50 μL. The thermocycling program for plasmid amplification was 95 °C for 1 min, 25 cycles of 95 °C for 30 s, 55 °C for 30 s, and 72 °C for 7 min, and a final extension at 72 °C for 10 min using an OpenPCR thermocycler (Chai Biotechnologies, Santa Clara, CA). After confirmation that the amplification succeeded by agarose gel electrophoresis, the methylated parental DNA strand was digested by addition of *Dpn*I (5 U) and incubation at 37 °C for 3 h. An aliquot of the reaction mixture (10 μL) was transformed into *E. coli* DH5α competent cells by heat shock. The transformed cells were spread on a lysogeny broth (LB) agar plate containing 100 μg/mL ampicillin and incubated at 37 °C overnight. Several resulting colonies were picked and grown overnight in liquid LB-ampicillin media (3 mL), and plasmid DNA was isolated using the QiaPrep MiniPrep kit. Sequencing of the entire SABP2 gene confirmed that it contained the desired mutations but no others.

Protein Expression and Purification. *E. coli* BL21 (DE3) containing pET21a(+)−SABP2 or the corresponding mutated plasmid were grown in modified TB media at 37 °C until the OD_{600} reached 1.4−1.6 and then cooled to 17 °C. Protein expression was induced by adding IPTG to a final concentration of 1 mM, the culture was shaken at 17 °C for 24 h, and the cells were harvested by centrifugation at 5000*g* for 15 min at 4 °C. Supernatants were discarded, and cells were resuspended in buffer A (50 mM sodium phosphate buffer, 300 mM NaCl, 20 mM imidazole, pH 8.2). The cells were lysed at 4 °C in an ice−water bath by ultrasound (Sonifier, output magnitude 40%, duty time 3 s, interval time 6 s, 8 min). The cell extract was centrifuged at 12000*g* at 4 °C for 30 min, and the supernatant was used for protein purification. The recombinant proteins contained C-terminal hexahistidine tags and were purified from the cell lysate by Ni-affinity chromatography (Ni-NTA, Qiagen) according to the manufacturer's instructions. Proteins were eluted in buffer B (50 mM sodium phosphate, 300 mM NaCl, 125 mM imidazole, pH 8.2), and then the buffer was exchanged to BES (*N*,*N*-bis(2-hydroxyethyl)-2-aminoethanesulfonic acid, 5 mM, pH 7.2) using 10000 MWCO Amicon Ultra spin concentrators (Millipore, Billerica, MA, USA).

Esterase Activity. Hydrolysis of *p*-nitrophenyl acetate (pNPAc) was measured at pH 7.2 and 24 °C and was corrected for spontaneous hydrolysis. The assay was performed in a 96-well microtiter plate with reaction volume of 100 μL (light path length = 0.29 cm) containing pNPAc (0.3 mM), 6.67 vol % acetonitrile, BES (4.2 mM, pH 7.2), and about 1 μg of enzyme. The release of *p*-nitrophenoxide (ε_{404nm} = 16600 M^{-1} cm^{-1}) was measured spectrophotometrically (SpectraMax Plus 384 plate reader, Molecular Devices, Sunnyvale, CA). Enzyme-catalyzed and spontaneous reaction rates were measured in triplicate and reported as the mean and standard

DOI: 10.1021/acs.biochem.5b00333
Biochemistry 2015, 54, 4330−4341

deviation. One unit of activity corresponds to 1 μmol of *p*-nitrophenoxide released per minute. Steady state kinetic constants were determined with the same method by varying the *p*-nitrophenyl acetate concentrations from 0 to 6 mM (6.67 vol % acetonitrile). Data was fit to the Michaelis−Menten equation by a nonlinear fit using Origin 7.5 (OriginLab, Northampton, MA, USA).

Thermodynamic Stability of Wild-type SABP2 and Variants. The unfolding of enzyme in increasing concentrations of urea (0−6.2 M) or guanidinium chloride (GdmCl) (0−4.5 M) was monitored by the decrease in intrinsic tryptophan fluorescence using SpectraMax GEMINI XS plus-384 plate reader (Molecular Devices, Sunnyvale, CA) with an excitation wavelength of 278 nm and an emission wavelength of 329 nm. Each well in the 96-well microtiter plate contained enzyme in BES buffer (20 μL, 5 mM buffer pH 7.2) with final protein concentration of 0.1−0.3 mg/mL, $(180 - x)$ μL of assay buffer (5 mM BES buffer, pH 7.2), and x μL of urea stock solution (8 M). Solutions were equilibrated at 4 °C for 16 or 24 h, then warmed to room temperature for 15 min before measuring the fluorescence. The relative concentrations of the folded or native conformation, *N*, and unfolded or denatured state, *U*, were determined by comparing the fluorescence at low urea concentrations (completely folded) and high urea concentrations (completely unfolded). The equilibrium ratio of folded and unfolded forms at a particular denaturant concentration yields the free energy of protein unfolding, ΔG, at that denaturant concentration, eq 1,

$$\Delta G = -RT \ln(U/N) \tag{1}$$

where R is the gas constant and T is the temperature. A plot of this free energy versus denaturant concentration yields a straight line of the form in eq 2,

$$\Delta G = \Delta G_{uw} - m[\text{urea}] \tag{2}$$

where m is the slope and ΔG_{uw} is the intercept. This intercept corresponds to the free energy of unfolding in the absence of denaturant.[18,42]

To study whether the loss of fluorescence correlated with a loss of esterase activity, we measured the esterase activity remaining after denaturation. Enzyme was incubated with denaturant for 16 h, and an aliquot (10 μL, ∼1 μg of enzyme) was removed and immediately added to the esterase activity assay solution (90 μL). The increase in absorbance at 404 nm was monitored as described above.

To measure the reversibility of unfolding, the enzyme was incubated with denaturant, and then the denaturant was removed by dialysis (10 kDa MW cut off, 3.5 L of BES buffer (5 mM, pH 7.2)) for total of 24 h, replacing with fresh buffer three times. The esterase activity of dialyzed enzyme was compared with the activity before incubation with denaturant.

Monitoring Unfolding at Two Wavelengths. To confirm the formation of an intermediate in the unfolding of SABP2, we measured the fluorescence intensity at different urea concentrations at two wavelengths: 320 nm (Y_{320}) and 365 nm (Y_{365}). If the folded protein (N) unfolds without a stable intermediate to the unfolded form (U), then the changes at the two wavelengths are proportional; a plot of Y_{320} versus Y_{365} is a straight line according to eq 3 (derivation and explanation by Bushmarina and colleagues[43]).

$$Y_{320} = a + bY_{365} \quad \text{where}$$
$$a = Y_{320}(\text{N}) - \frac{Y_{320}(\text{U}) - Y_{320}(\text{N})}{Y_{365}(\text{U}) - Y_{365}(\text{N})} Y_{365}(\text{N}) \quad \text{and}$$
$$b = \frac{Y_{320}(\text{U}) - Y_{320}(\text{N})}{Y_{365}(\text{U}) - Y_{365}(\text{N})} \tag{3}$$

$Y_{320}(\text{N})$ represents the fluorescence intensity at 320 nm due to the folded form and $Y_{365}(\text{U})$ represents the fluorescence intensity at 365 nm due to the unfolded form. Several groups have used this two-wavelength approach, first described by Burstein, to detect intermediates in protein unfolding, although they typically use a simple two line fit to the data.[43−46] This two-line method assumes that there is no overlap between transitions and no points where a significant portion of protein is in more than two states. The nonlinear solution method used here allows for overlap between transitions.

Extending eq 2 to a three-state model yields eqs 4 and 5 where ΔG_{ni} is the free energy of native to intermediate transition and ΔG_{iu} the free energy for the transition of intermediate to unfolded.

$$\Delta G_{ni} = RT \ln K_{ni} = \Delta G_{niuw} - m_{ni}[\text{urea}] \tag{4}$$

$$\Delta G_{iu} = RT \ln K_{iu} = \Delta G_{iuuw} - m_{iu}[\text{urea}] \tag{5}$$

The free energy of each transition in pure water is ΔG_{niuw} and ΔG_{iuuw} and K_{ni} is the ratio of protein in the native and intermediates states, while K_{iu} is the ratio of protein in the intermediate and unfolded states. The m values for the two transitions (m_{ni} and m_{iu}) are the susceptibility of native and intermediate states to the denaturant such as urea. These equations predict the fluorescence (Y) at a particular wavelength and concentration of denaturant from the parameters of fluorescence of each state (Y_i, Y_n, and Y_u), eq 6.

$$Y = \frac{K_{iu}Y_u + \frac{Y_n}{K_{ni}} + Y_i}{K_{iu} + 1 + \frac{1}{K_{ni}}} \tag{6}$$

Minimization of the squared residuals between measured and calculated fluorescence using the nonlinear "Solver" add-in with Microsoft Excel yielded values for ΔG_{niuw}, ΔG_{iuuw}, and Y_i for both wavelengths. To reduce the number of variables and prevent over fitting of data, m values of each domain of SABP2 were calculated using solvent accessible surface area (ProtSA[47]) using the relationship described by Myers and colleagues.[48] The calculated m value for the catalytic domain was 1938 kcal/(mol·M), and that for the cap domain was 897 kcal/(mol·M). Y_n and Y_u were the average of the three highest or lowest fluorescence readings. The 95% confidence intervals of ΔG_{niuw}, and ΔG_{iuuw} values were calculated as described by Kemmer and Keller.[49] We used the "FINV" function in Microsoft Excel to find the range of squared residuals within the 0.95 confidence range given the degrees of freedom. ΔG_{niuw} and ΔG_{iuuw} were then varied and held constant while other variables were recalculated using Solver to determine the range of ΔG_{niuw} and ΔG_{iuuw} values that produced squared residuals within the calculated confidence range.

Heat Stability of Wild-type SABP2 and Variants. The kinetic stability was determined by measuring the residual enzymatic activity at room temperature after 15 min incubation (BES buffer, 5 mM, pH 7.2) at elevated temperatures. The temperature at which 50% of the enzymatic activity is lost after

DOI: 10.1021/acs.biochem.5b00333
Biochemistry 2015, 54, 4330−4341

15 min incubation, $T_{1/2}^{15min}$, was determined by fitting the loss of activity at different temperatures to a four-parameter Boltzmann sigmoidal function ($y = a + (b - a)/(1 + e(x - x_0)/k)$) using Origin 7.5 (Origin Software Inc., Northampton, MA, USA). Half-life at 60 °C was calculated from the activity loss after 15 min incubation with the function 15 ln(2)/ln(unheated/heated). This temperature is low enough to retain some activity for the wild-type enzyme but high enough to see some loss of activity for the stabilized variants.

The heat denaturation of SABP2 was also measured by the loss of circular dichroism (CD) signal (JASCO J-815 spectropolarimeter with Peltier-type temperature controller (PTC-348WI)) at 224 nm upon heating the sample from 20 to 90 °C at 2 °C min^{-1}. $T_{1/2}^{CD}$ is the temperature at which 50% of the signal is lost. CD measurements were made at a protein concentration of 0.2−0.3 mg/mL in BES buffer (5 mM, pH 7.2) with a 1 mm path length cell. The wavelength of 224 nm is a local minimum in the CD spectrum of SABP2 that showed the largest changes upon heating. Signals due to both α-helix and β-sheet structures typically appear in this region. The data were normalized to the lowest signal observed at 224 nm.

Computational Methods. The FoldX algorithm (version 3.0 beta5.1, available from http://foldx.crg.es/) modeled protein stability for various amino acid replacements using empirically weighted energy terms.[50] The X-ray structure of SABP2 (pdb 1Y7I[33]) was preprocessed using "RepairPDB" command to minimize the energy of the structure, followed by the "BuildModel" command to evaluate the effect of various substitutions.

The molecular dynamics (MD) simulation was performed using the software NAMD[51] using 64 Pentium IV processors running Ubuntu Linux starting from the X-ray crystal structure of SABP2 (pdb 1Y7I,[33] chain A). First, the structure was prepared for the simulation by adding hydrogen atoms and replacing the water molecules in the structure by a water sphere with a radius of 10 Å and centered at the protein's center of mass. The geometry of this model was optimized by 1000 steps of energy minimization. Next, the molecular dynamics simulation modeled 2 ns of enzyme motion at 310 K and 1.013 bar, which required ∼48 h of calculation time. The simulation results were visualized using the VMD molecular graphics program.[52] The root-mean-square deviation (RMSD) and root-mean-square fluctuation (RMSF) values for backbone atoms were calculated and compared with the experimental RMSF value, which can be derived from the crystallographic *B*-factors (*B*, temperature factor) according to eq 7.[53,54]

$$\mathrm{RMSF}^2 = \frac{3B}{8\pi^2} \tag{7}$$

RESULTS

Reversible Denaturation in Urea or GdmCl Solutions. Incubation of wild-type SABP2 for 24 h at 4 °C in solutions of increasing urea concentration caused a decrease of the fluorescence at 329 nm, Figure 3A. This decrease is consistent with protein unfolding to expose the indole ring of tryptophan to solvent, which quenches the fluorescence. SABP2 contains four tryptophan residues: Trp20 is completely buried within the catalytic domain, Trp131 is mostly buried within the cap−catalytic domain interface, Trp18 is buried within the cap−catalytic domain interface as well as contacting the cap domain from the other monomer, and Trp220 is partially solvent exposed within the catalytic domain, Figure 2. Changes in the environment of these tryptophans decreases the fluorescence, but assigning this decrease to specific changes in structure is impossible because there are four tryptophans each with multiple possible conformations and overlapping electronic states. The midpoint of the decrease in fluorescence, which corresponds to equal amounts of folded and unfolded protein, occurred at 2.3 M urea. The slight increase in fluorescence at 0.5−1.0 M urea suggests a small conformational change, but the details of this change are unknown.

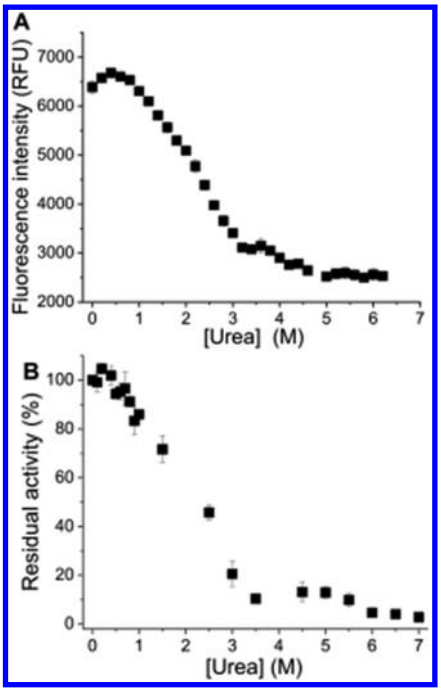

Figure 3. Unfolding of wild-type SABP2 (0.3 mg/mL) in urea solutions. (A) Tryptophan fluorescence at 329 nm decreased after incubation of SABP2 in increasing concentrations of urea. The midpoint for the decrease occurred at ∼2.3 M urea. RFU = relative fluorescence units. (B) Esterase activity (*p*-nitrophenyl acetate hydrolysis) also decreased in increasing concentrations of urea. The midpoint for the decrease occurred at ∼2.4 M urea. Samples were incubated in urea solution, transferred to assay solution without urea, and immediately assayed. The points in both panels represent the mean ± standard deviation (SD) of three independent samples.

The denaturation in urea also decreased the hydrolytic activity (hydrolysis of *p*-nitrophenyl acetate), but this decrease was reversible. When the hydrolytic activity was measured immediately after removing an aliquot from the urea solution, the midpoint of the decrease in enzymatic activity occurred at 2.4 M urea, Figure 3B, similar to the midpoint of the fluorescence decrease. Unfolding in urea required hours (data not shown), so the refolding is similarly slow since the ratio of the forward and reverse rates corresponds to the equilibrium constant. The ∼5 min required for the assay is not enough time to refold significant amounts of protein. However, when the hydrolytic activity was measured after removing the urea by dialysis over 24 h, most (78%) of the original esterase activity was recovered, Table S2, Supporting Information. This recovery indicates that the loss of hydrolytic activity is reversible by refolding of the protein. The incomplete recovery may be due to misfolding, aggregation, or the formation of non-native disulfide links during the refolding. SABP2 contains five cysteine residues, none of them as disulfide links.

DOI: 10.1021/acs.biochem.5b00333
Biochemistry 2015, 54, 4330−4341

SABP2 also unfolded in solutions of guanidinium chloride (GdmCl) but at lower concentrations compared with urea, Figure S1, Supporting Information. The midpoint of unfolding occurred at 0.80 M GdmCl according to both the decrease in tryptophan fluorescence and the decrease in hydrolytic activity. While both urea and GdmCl disrupt hydrogen bonding, GdmCl also disrupts electrostatic interactions and shows a stronger unfolding effect toward most proteins.[17]

Unfolding Involves a Least One Intermediate. The changes in maximum fluorescence wavelength show a different pattern from the changes in fluorescence intensity described above. Buried tryptophan residues typically fluoresce maximally at 330 nm, while solvent exposed tryptophans fluoresce maximally at 350 nm.[33] Thus, one expects the wavelength of the fluorescence maximum to shift from 330 to 350 nm as the protein unfolds. Indeed, this shift occurs for SABP2, but the midpoint for this shift occurs not at 2.1−2.4 M urea where the fluorescence intensity at 329 nm decreases and the hydrolytic activity is lost, but between 4 and 5 M urea, Figure 4A. Unfolding in GdmCl shows similar behavior, Figure S2, Supporting Information. The midpoint for the decrease in fluorescence intensity at 329 nm occurred at 0.8 M GdmCl, but the midpoint for the shift in fluorescence wavelength occurred between 1.5 and 2.0 M GdmCl. A closer look at the unfolding curves in Figure 2A shows a second, smaller change in fluorescence intensity between 4 and 5 M urea and in Figure S1A, Supporting Information, a second change between 1.5 and 2.0 M GdmCl. The existence of two transitions indicates that unfolding of SABP2 involves at least one intermediate state.

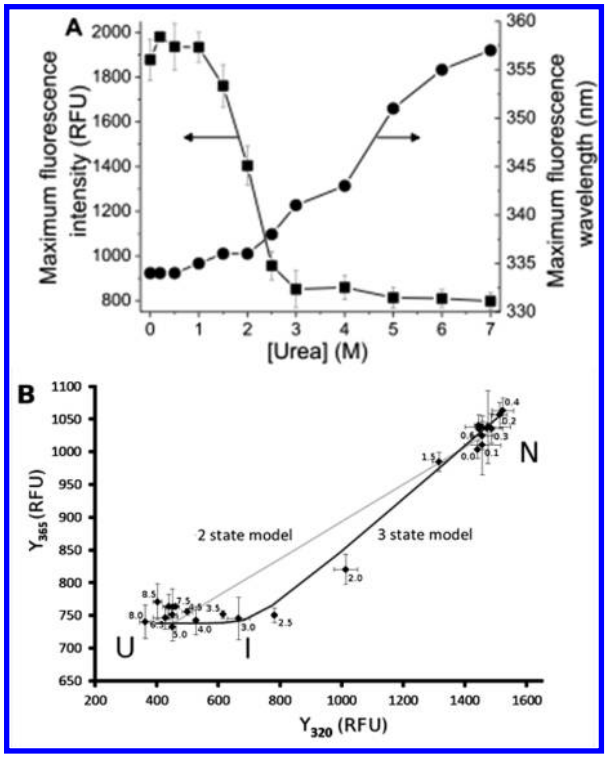

Figure 4. Unfolding of wild-type SABP2 (0.1 mg/mL) involves a folding intermediate. (A) Unfolding of SABP2 shows two transitions. The maximum tryptophan fluorescence intensity drops at ∼2.3 M urea (left scale and curve; same data as in Figure 1A), but the shift in the wavelength of emission occurs at ∼5 M urea (right scale and curve). The lines connecting the data points serve only to guide the eye. (B) Unfolding monitored at two wavelengths simultaneously. The intensity of fluorescence at 320 nm (Y_{320}) and at 365 nm (Y_{365}) changes linearly if the folded protein (N) unfolds directly to the unfolded form (U) but changes nonlinearly if it unfolds via a stable intermediate (I). Numbers near the symbols indicate the urea concentrations of the measurement. The nonlinear, three-state model (darker line) fits the data better than the linear, two-state model (lighter line). Each point represents the mean ± SD from three independent samples.

Another way to show that unfolding involves an intermediate is to monitor the fluorescence changes at two wavelengths. If the native protein unfolds directly to the denatured form, then the fluorescence changes at all wavelengths should be linear. If they are not linear, then unfolding involves at least one intermediate. A plot of fluorescence intensity at 320 nm versus fluorescence intensity at 365 nm was not linear indicating at least one intermediate state, Figure 4B. A plot of unfolding in GdmCl also showed similar, but less pronounced, nonlinear behavior, Figure S2B, Supporting Information.

Free Energies of Unfolding. If protein unfolding occurs in one step (two states), the denaturant-induced shifts in the equilibrium constant can be extrapolated to 0 M denaturant to yield the unfolding free energy of the protein in water, ΔG_{uw}, see eq 2 above. Although we know that unfolding of SABP2 involves an intermediate, we nevertheless fit the data to the one-step model, which yielded an unrealistically low value of 2.4 kcal/mol, Figure S3, Supporting Information. Unfolding free energies of proteins similar in size to SABP2 typically range from 5 to 15 kcal/mol.[34−36] This low value is typical for much smaller proteins of 50−70 amino acids. Using a one-step model in cases involving intermediates underestimates the true unfolding free energy.[37]

Fitting the data to a two-step unfolding model (three states) yielded a free energy of unfolding of SABP2 in water of 6.9 ± 1.5 kcal/mol. The two-step unfolding model includes the relative amounts of folded, unfolded, and intermediate states at various urea concentrations (eqs 4 and 5) and extrapolates these values to 0 M urea. The slope of the lines is the constant *m*, which indicates the susceptibility of the protein to urea-induced unfolding. To avoid overfitting of the data, values of *m* were calculated from the surface area of the protein domains. The two-step model fit the fluorescence data more closely than the one-step model. The sum of squared residuals was 65% lower for the two-step model, Figure S3, Supporting Information. This two-step model yielded a free energy of unfolding of 3.5 ± 0.5 kcal/mol for the first transition (catalytic domain) and a similar 3.4 ± 1.0 kcal/mol for the second transition (cap domain), Table 1. The sum of the two values, 6.9 ± 1.5 kcal/mol is the free energy of unfolding of SABP2 in water. This value is similar to cutinase, a similarly sized enzyme from a mesophile, but lower than that for esterases from thermophiles, Table 1 above.

The *m*-values in the two-step unfolding model assumed that the first unfolding corresponds to the catalytic domain and the second unfolding corresponds to the cap domain. Reversing this assumption resulted in a poorer fit, with a sum of squared residuals 110% higher. This assumption is also consistent with substitutions in the catalytic domain causing changes in the first transition, see below. The larger domain unfolds first because it is more sensitive to urea.

Unfolding of SABP2 in GdmCl did not yield an estimate for the unfolding free energy in water. The unfolding also involves an intermediate, but the two steps are not sufficiently separated to measure the fluorescence properties of the intermediate.

DOI: 10.1021/acs.biochem.5b00333
Biochemistry 2015, 54, 4330−4341

Fitting to the three-state model was not possible without this data.

Heat-Induced Denaturation. Heating a sample of wild-type SABP2 at 1 °C/min while monitoring the circular dichroism (CD) signal at 224 nm showed a loss of signal as the protein unfolded. The midpoint for the change ($T_{1/2}^{CD}$) occurred at 49.0 ± 0.3 °C, Figure 5A. Similarly, incubation of

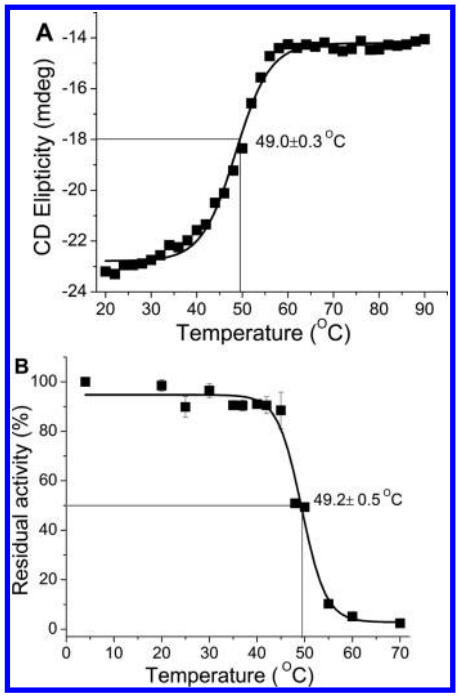

Figure 5. Heat-induced denaturation of wild-type SABP2. (A) Loss of negative CD signal at 224 nm upon heating SABP2 at 1 °C/min. The fit to a two-state unfolding indicates a melting temperature of 49.0 ± 0.3 °C. (B) Incubation of SABP2 (0.2 mg/mL) at elevated temperatures for 15 min, followed by cooling to room temperature, decreased the catalytic activity. The temperature where half the activity was lost ($T_{1/2}^{15min}$) was 49.2 ± 0.5 °C. The line is a best fit to a sigmoidal function.

wild-type SABP2 at elevated temperature for 15 min followed by cooling to room temperature decreased the catalytic activity, Figure 5B. This experiment measures the irreversible heat-induced unfolding. The midpoint for the decrease ($T_{1/2}^{15min}$) was the same to within experimental error as for the CD measurement, 49.2 ± 0.5 °C. Thus, the heat-unfolded protein does not refold quickly upon cooling. The half-life at 60 °C was 3.5 min. Both transitions appear smooth with no suggestion of an intermediate state. The protein remains mostly soluble even above the transition temperature (Figure S4, Supporting Information), although the soluble inactive form may partly aggregate.

Selecting Locations for Proline Substitutions. We chose locations for the proline substitutions in two different ways. The first was amino acid sequence comparison with a more stable homologue. Locations where the homologue has a proline residue should also accommodate a proline residue in the corresponding location of SABP2. The homologue chosen was hydroxynitrile lyase from *Manihot esculenta* (*Me*HNL). Both SABP2 and *Me*HNL are plant enzymes, they share 41% identical amino acid residues, and both structures show an α/β-hydrolase fold where their main chains overlay with an rmsd of 0.75 Å, Figure S5, Supporting Information. *Me*HNL is much more stable than SABP2.[31,32] Its half-life at 50 °C (2.7 h) is more than ten times longer than that of SABP2. The temperature of heat induced unfolding as measured by circular dichroism spectroscopy ($T_{1/2}^{CD}$), 69.3 °C, is 20 °C higher than that for SABP2. Alignment of the structures and amino acid sequences of SABP2 and *Me*HNL identified six locations where *Me*HNL contains a proline residue but SABP2 does not: L46, S70, S115, K190, E215, and V227, Figure S5, Supporting Information. All six of these substitutions were tested. Although the esterases from thermophiles in Table 1 are more stable than *Me*HNL, they share only 14−16% amino acid identity with SABP2, so the structures match less well to SABP2.

The second way to choose locations for proline substitutions was to add them in flexible regions within SABP2 because these regions should be able to accommodate the main chain conformations required by proline. One disadvantage of this approach is that introducing the proline in a flexible region will reduce its flexibility. Reducing the flexibility of the folded form decreases its entropy and stability, but we expected that this decrease would be smaller than the effect on the unfolded form. Other researchers have stabilized α/β-hydrolases by targeting random substitutions to the most flexible regions of proteins.[60,61] Our approach also targets the flexible regions, but only considers proline residues as replacements.

The *B*-factors from the X-ray crystal structure of SABP2, determined at 100 K, show low average flexibility, Figure 6 and Figure S6, Supporting Information. Flexible regions include the N- and C-termini, a region in the cap domain (residues 140−145), and two regions in the catalytic domain (residues 66−73 and 180−203). A molecular dynamics simulation at 310 K

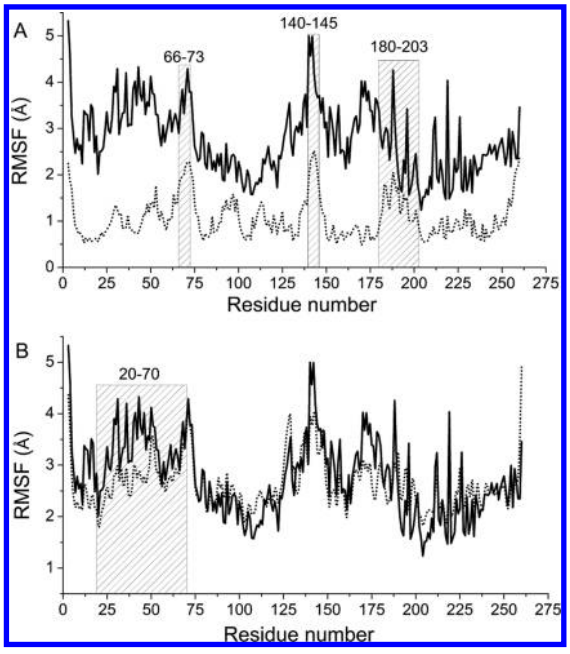

Figure 6. Flexibility of wild-type SABP2 and SABP2-L46P-S70P. (A) The three most flexible regions of wild-type SABP2 are the catalytic domain residues 66−73 and 180−203 and cap domain residues 140−145. These regions show the highest root-mean-square fluctuation (RMSF) of the backbone atoms in both X-ray crystallography at 100 K (dotted line) and molecular dynamics simulation at 310 K (solid line). (B) The region of residues 20−70 (boxed) is more flexible in wild-type SABP2 (solid line) than in SABP2-L46P-S70P (dotted line) according to molecular dynamics simulation at 310 K.

DOI: 10.1021/acs.biochem.5b00333
Biochemistry 2015, 54, 4330−4341

Table 2. Steady-State Kinetic Constants[a] and Stability of SABP2 Variants with Added Proline Residues

SABP2	k_{cat} (s^{-1})	K_M (mM)	k_{cat}/K_M (mM^{-1} s^{-1})	$\Delta C_{1/2}^{urea}$[b] (M)	$T_{1/2}^{60°C}$[c] (min)	$T_{1/2}^{15min}$[d] (°C)	$\Delta T_{1/2}^{15min}$ (°C)
WT	1.82 ± 0.02	2.24 ± 0.05	0.81		3.50 ± 0.03	49.2 ± 0.5	
L46P cat	2.44 ± 0.12	3.10 ± 0.23	0.79	+0.2	10.2 ± 1.3	55.6 ± 0.4	+6.4
S70P cat	1.88 ± 0.08	3.10 ± 0.28	0.61	+0.1	7.1 ± 0.2	54.6 ± 0.4	+5.4
S115P cap	0.89 ± 0.04	1.85 ± 0.23	0.48	−0.3	12 ± 1.7	51.0 ± 0.9	+1.8
S141P cap	1.56 ± 0.05	1.60 ± 0.11	0.97	+0.0	9.4 ± 0.3	54.1 ± 0.8	+4.9
K190P cat	1.30 ± 0.07	3.21 ± 0.35	0.41	−1.5	<2	42.2 ± 0.7	−7.0
E215P cat	2.68 ± 0.20	3.49 ± 0.38	0.77	+0.9	5.3 ± 0.1	53.4 ± 0.5	+4.2
V227P cat	2.51 ± 0.21	4.42 ± 0.45	0.79	−0.4	<2	46.9 ± 0.7	−2.3
L46P−S70P cat−cat	2.18 ± 0.06	2.44 ± 0.15	0.89	+0.1	22.5 ± 1.7	74.9 ± 1.7	+25.7
L46P−S141P cat−cap	2.29 ± 0.16	3.03 ± 0.30	0.76	−0.1	11.7 ± 0.1	55.8 ± 0.4	+6.6
S70P−S141P cat−cap	3.42 ± 0.07	3.77 ± 0.15	0.91	−0.2	16.0 ± 0.5	60.5 ± 0.4	+11.3
L46P−S70P−E215P cat−cat−cat	2.34 ± 0.13	6.00 ± 0.56	0.39	+0.9	17.5 ± 0.5	57.2 ± 0.4	+8.0
L46P−S70P−S141P cat−cat−cap	2.05 ± 0.10	2.74 ± 0.10	0.75	+0.0	14.4 ± 0.2	59.6 ± 0.8	+10.4

[a]Hydrolysis of *p*-nitrophenyl acetate at pH 7.2. [b]Change in the concentration of urea where the protein was half unfolded as measured by protein fluorescence at 329 nm (24 h incubation at 4 °C in 5 mM BES (pH 7.2), 0.1−0.3 mg protein/mL). This unfolding corresponds the first transition, tentatively assigned to an unfolding of the catalytic domain. Positive values indicate increased stability. [c]Half-life for activity loss at 60 °C. [d]Figure S5 in Supporting Information shows the heat denaturation curves.

showed a higher average flexibility and a similar pattern. Regions 66−73 and 140−145 remain flexible, but the 180−203 region shifts to 160−180 and a region 30−60 also appears flexible. We targeted the proline substitutions to the three flexible regions identified by *B*-factors. The sequence comparison above already suggested proline substitutions in two of the regions: S70 and K190.

Among the six amino acid residues in the third flexible region (140−145), residues 142 and 145 are already proline. FoldX, sofware for modeling protein stability, predicted that a proline substitution at G140, E143, or E144 would destabilize the protein but a substitution at S141 would stabilize the protein, Table S3, Supporting Information. We chose the S141P substitution. The total of predicted locations for substitution is seven: six from sequence alignment and three from targeting flexible regions, but two predictions are common to both methods.

Single Proline Substitutions Increase Stability of SABP2. Site-directed mutagenesis created seven variants, each with a different single proline substitution. After expression of the proteins in *E. coli* and purification by Ni-affinity chromatography, SDS-PAGE analysis showed pure proteins.

The steady state kinetic constants for the single proline substitution variants were within a factor of 2 of those for wild-type SABP2, Table 2. The average k_{cat}/K_M values were 0.7 ± 0.2 mM^{-1} s^{-1} compared with 0.81 mM^{-1} s^{-1} for wild-type SABP2. The largest changes for the k_{cat}/K_M value were a decrease by a factor of 2 to 0.41 mM^{-1} s^{-1} for K190P and an increase by a factor of 1.2 to 0.97 mM^{-1} s^{-1} for S141P. The largest changes in k_{cat} value were a decrease by a factor of 2 for S115P and an increase by a factor of 1.5 for E215P. The largest changes in K_M value were a decrease by a factor of 1.4 for S141P and an increase by a factor of 2 for V227P.

The increase in the concentration of urea needed to unfold half of the protein ($\Delta C_{1/2}^{urea}$) indicated an increase in stability, Table 2. Due to the complexities of the unfolding, we did not convert these values to free energies. Variant E215P showed the largest increase in stability, $\Delta C_{1/2}^{urea}$ = +0.9 M, while variant K190P showed the large decrease in stability, $\Delta C_{1/2}^{urea}$ = −1.5 M. Both of these substitutions were in the catalytic domain suggesting that this first unfolding transition unfolds the catalytic domain. The changes for the other five variants were smaller, ranging from $\Delta C_{1/2}^{urea}$ = +0.4 to −0.4 M. The average absolute effect on urea tolerance for mutations in the catalytic domain was larger (0.62 ± 0.52 M urea) than that for mutations in the cap domain (0.15 ± 0.21 M urea).

The proline substitutions also increased the heat inactivation temperatures, $T_{1/2}^{15min}$, but the best variant differed from that identified by denaturation in urea. The largest increase in heat inactivation temperature was +6.4 °C for L46P, and the second best, +5.4 °C, was S70P. Both these substitutions are in the catalytic domain. Similarly, the half-lives at 60 °C more than doubled for L46P and S70P, as well as for S115P and S141P. The worst variant was K190P, with a temperature decrease of 7.0 °C and half-life of under 2 min at 60 °C. Variant K190P was also the worst one as measured by urea denaturation. This location was predicted by both targeting flexible regions and the sequence alignment.

Substitutions in the catalytic domain cause the largest increases and decreases in the first unfolding transition, thus identifying this transition as the unfolding of the catalytic domain, Figure 2. The two substitutions in cap domain had little effect on urea-induced unfolding. $\Delta C_{1/2}^{urea}$ was unchanged for S141P and decreased by 0.3 M for S115P indicating a slight destabilization. Two of the substitutions that targeted flexible regions (S70P and S141P) had little effect on the equilibrium in urea ($\Delta C_{1/2}^{urea}$ = +0.1 and 0.0 M, respectively), possibly because they reduce flexibility in both the folded and unfolded conformations. These two substitutions stabilized SABP2 to heat inactivation ($\Delta T_{1/2}^{15min}$ = +5.4 and +4.9 °C and half-lives of 12.0 and 9.4 min at 60 °C, respectively), possibly by reducing aggregation.

Multiple Proline Substitution Variants. Combining stabilizing proline substitutions did not further increase stability as measured by urea denaturation but did increase stability dramatically as measured by heat inactivation, Table 2 and Figure S7, Supporting Information. The most stable multiple substitution variant as measured by urea unfolding was L46P−S70P−E215P, but it was no more stable than E215P. The most stable multiple substitution variant as measured by heat inactivation was L46P−S70P with a $T_{1/2}^{15min}$ of 74.9 ± 1.7 °C, which is a dramatic 25.7 °C higher than wild-type SABP2, and a half-life at 60 °C more than six times longer than wild-type protein. Both substitutions are in the catalytic domain.

DOI: 10.1021/acs.biochem.5b00333
Biochemistry 2015, 54, 4330−4341

Molecular dynamics simulation of SABP2-L46P-S70P folded conformation showed less flexibility in region 20−70 than wild-type, Figure 4B.

DISCUSSION

Unfolding of most α/β-hydrolases involves intermediates, but in a few cases unfolding occurs in a single step (cutinase, esterases from thermophiles). The unfolding of SABP2 in urea was unusual because the intermediate can be clearly distinguished by fluorescence. The first unfolding transition affects fluorescence at 365 nm, while both the first and second transitions affect the fluorescence at 320 nm. Fitting these changes to a three state model yields a free energy of unfolding of 3.4 kcal/mol for the first transition and 3.5 kcal/mol for the second. The total, 6.9 kcal/mol, is typical for an α/β-hydrolase from a mesophile.

The two unfolding steps likely correspond to the separate unfolding of the two domains; surprisingly we found that the catalytic domain is probably the first to unfold. Multidomain proteins often unfold via intermediates where one domain is mostly unfolded while the other domain is still predominantly folded.[40] While other possibilities cannot be ruled out, our data is consistent with one domain of SABP2 unfolding first, followed by the other domain. The loss of catalytic activity during the first unfolding is consistent with either domain unfolding since both domains contribute to the substrate binding site and disrupting of either would be expected to disrupt catalysis. To fit the fluorescence changes upon unfolding best required m values predicted by the surface areas of the two domains with the catalytic domain corresponding to the first transition and the cap domain corresponding to the second transition. Substitutions within the catalytic domain have a large effect on the first transition, while substitutions within the cap domain have little effect. These results are also consistent with the first transition corresponding to the unfolding of the catalytic domain.

Heat induced inactivation showed no evidence for an intermediate. The unfolding by heat disrupts solvation and favors flexible unfolded forms, while unfolding with denaturant disrupts hydrogen bonding. It is possible, even likely, that urea-induced denaturation and heat-induced denaturation generate different unfolded proteins, so that changes to increase stability may affect the two measures differently.

Locations for proline substitution were chosen based on an amino acid sequence alignment between SABP2 and *Me*HNL. This approach showed a good success rate to stabilize against urea denaturation: (3/6 = 50%): substitutions L46P, S70P, and E215P. The success rate was slightly better in stabilizing against heat inactivation (4/6 = 67%): substitutions L46P, S70P, S115P, and E215P, Table 3. The three substitutions in the catalytic domain stabilized against both conditions consistent with notion that it unfolds in both conditions, while the substitution in cap domain only stabilized against heat denaturation consistent with the notion that the cap domain does not unfold first in urea.

Adding proline to flexible regions had a similar success rate. This approach suggested three substitutions: S70P, S141P, and K190P, where S70P and K190P were also predicted by the sequence alignment. For urea denaturation, only S70P stabilized SABP2 (33% success), while for heat inactivation, both S70P and S141P stabilized SABP2 (67% success), Table 3. This approach required more effort, an X-ray crystal structure to identify the flexible regions and some computation to predict which location in these regions would be best.

Table 3. Success of Methods To Choose Location for Proline Substitution To Increase the Heat Stability of SABP2

	method[a]		
mutation	copy	flexibility	structure[b]
L46P	+++		
S70P	++	++	(++)[c]
S115P	+		+
S141P		++	
K190P	− − −	− − −	
E215P	++		++
V227P	−		
success rate	4/6	2/3	2/2

[a]Entries show change in $T_{1/2}^{15min}$: +++ > 6 °C, ++ = 3−6 °C, + = 0−3 °C, − = −3 to 0, − − = −3 to −6, − − − < −6. [b]Analysis of SABP2 secondary structure predicted 34 possible locations for a proline substitution. Only two of these, S115P and E215P, were also predicted by other methods. [c]In SABP2, residue 70 does not have a secondary structure that accommodates proline, but its conformation may change to the type II β turn conformation found in *Me*HNL, which can accommodate proline.

Analysis of the secondary structure can also suggest locations for a proline,[36,64] but we did not use this approach because it ignores the surrounding structure. Proline often occurs at the i + 1 position of type I β-turns, at the i position in type II β-turns, as the N-terminal residue of α helices, and sometimes in other turn positions if the ψ angle is near −60°. Analysis of the SABP2 structure using program PROMOTIF through PDBsum (http://www.ebi.ac.uk/pdbsum/) identified 39 locations predicted to fit a proline residue.[39] Five of these already contain a proline, and three more were excluded because they are within 4 Å of the bound product, leaving 31 possible locations, Table S4, Supporting Information. Two locations predicted above, S115 and E215, are among these 31. S115 is at the i + 1 position of a type I β turn, and E215 is at the N-cap of an α helix. Both of these substitutions stabilized the protein. The other five predicted locations are not among the 31. Two of these destabilized the protein, but three stabilized it, corresponding to an overall success of 4/7 = 57%. For example, residue V227 does not fit because it is in the i position of a type VIII β turn and location 141 is at the i position of a type I β turn. Location S70 may be a special case. Although it does not fit in SABP2 because it is at the i position of type I β turn, in *Me*HNL this location is a type II β turn, so substituting a proline may switch the conformation of the turn.

Our success with the structure approach (57%) is similar to that found by others. Using structural analysis, Prajapati and colleagues[65] found 4 of 7, 0 of 1, and 2 of 4 proline substitutions (50% overall) increased thermal stability in the proteins leucine−isoleucine−valine binding protein, ribose binding protein, and thioredoxin, respectively. A meta analysis of all reported proline substitutions in the Protherm database[66] found 33 proline substitutions in 10 proteins; 16 of these (48%) increased thermal stability. Thus, the success of the structure approach matches the average of all approaches.

Homologue comparison was more successful for SABP2 (67%), and others also reported high success rates. For example, Watanabe and colleagues[36] found 7 of 9 proline substitutions (78%) copied from a thermostable homologue increased stability of oligo-l,6-glucosidases. The improved

DOI: 10.1021/acs.biochem.5b00333
Biochemistry 2015, 54, 4330−4341

success rate when copying from homologues suggests that structure analysis predicts the fit of proline replacements poorly, likely because it considers only secondary structure while ignoring the surrounding regions. Homologue comparison may be more successful because it adds information from evolutionary history. Destabilizing proline substitutions will be selected against; for that reason identifying proline locations in homologues may be more reliable.

Combining the substitutions yielded a variant (L46P−S70P) that was dramatically stabilized to heat inactivation but no more stable to urea denaturation. The urea stability of the double and triple mutants tested was always less than the sum of the single mutants, and usually less than the single constituent mutants, while the thermal stability was close to additive and always greater than the individual mutations. Two possible hypotheses for this behavior are (1) thermal stability is measured at much higher temperature than chemical denaturation and (2) hydrogen bonds to the denaturant, not flexibility of the unfolded form, may drive unfolding due to chemical denaturation. Proline substitutions change the entropic advantage of unfolding and have little effect on hydrogen bonds to the denaturant. The stabilizing effect of proline substitution should be higher at higher temperatures because the entropy contribution to free energy increases a higher temperature. If hydrogen bond changes drive the unfolding in urea and guanidinium, then proline substitutions are not expected to stabilize the proteins since proline substitution does not affect hydrogen bonding. Others also reported that proline substitution improved thermal stability more than resistance to chemical denaturation.[65,67]

Despite the complexities of unfolding in multidomain proteins like α/β hydrolases, the proline substitution approach is a reliable way to stabilize SABP2, especially to heat, and may be useful for other α/β hydrolases. Choosing locations by aligning amino acid sequences with a stable homologue is the easiest approach. Choosing substitutions in flexible regions was also successful but relied on an X-ray structure. Stabilization to urea denaturation required substitutions in the catalytic domain, while stabilization to heat inactivation could be in either domain but was most successful in the catalytic domain.

■ ASSOCIATED CONTENT

Supporting Information

Primers used to create proline substitutions, reversibility of esterase activity loss in urea, folding free energy differences between wild-type and variant SABP2, locations compatible with proline substitution, unfolding of wild-type SABP2 in GdmCl solutions, fluorescence changes in SABP2 induced by urea matched to the three-state unfolding model, solubility of heat inactivated SABP2, amino acid sequence and crystal structure alignment of SABP2 and hydroxynitrile lyase from cassava, regions of higher flexibility in SABP2, and thermal inactivation of SABP2 variants. This material is available free of charge online at The Supporting Information is available free of charge on the ACS Publications website at DOI: 10.1021/acs.biochem.5b00333.

■ AUTHOR INFORMATION

Corresponding Author

*Phone: +1-612-624-5904. E-mail: rjk@umn.edu.

Author Contributions

‡J.H. and B.J.J. are co-first authors.

Funding

The authors acknowledge funding from U.S. National Science Foundation (Grants CBET-0932762, CHE-1152804), U.S. National Institutes of Health (Grants 1R01GM102205-01 and 5T32 GM08347), and China National Natural Science Foundation (Grant 31470793; fellowship to J.H.).

Notes

The authors declare no competing financial interest.

■ ACKNOWLEDGMENTS

We thank the Minnesota Supercomputing Institute for use of computers and software.

■ REFERENCES

(1) Pace, C. N. (1973) The stability of globular proteins. *Crit. Rev. Biochem. Mol. Biol. 3*, 1−43.

(2) Taverna, D. M., and Goldstein, R. A. (2002) Why are proteins marginally stable? *Proteins: Struct., Funct., Genet. 46*, 105−109.

(3) Fersht, A. R., and Serrano, L. (1993) Principles of protein stability derived from protein engineering experiments. *Curr. Opin. Struct. Biol. 3*, 75−75.

(4) Bloom, J. D., Raval, A., and Wilke, C. O. (2007) Thermodynamics of neutral protein evolution. *Genetics 175*, 255−266.

(5) Richardson, T. H., Tan, X., Frey, G., Callen, W., Cabell, M., Lam, D., Macomber, J., Short, J. M., Robertson, D. E., and Miller, C. (2002) A novel, high performance enzyme for starch liquefaction. Discovery and optimization of a low pH, thermostable α-amylase. *J. Biol. Chem. 277*, 26501−26507.

(6) Haddar, A., Agrebi, R., Bougatef, A., Hmidet, N., Sellami-Kamoun, A., and Nasri, M. (2009) Two detergent stable alkaline serine-proteases from *Bacillus mojavensis* A21: Purification, characterization and potential application as a laundry detergent additive. *Bioresour. Technol. 100*, 3366−3373.

(7) Tao, J. (Alex), Lin, G.-Q., and Liese, A. (2009) *Biocatalysis for the Pharmaceutical Industry: Discovery, Development, and Manufacturing*, John Wiley & Sons, Singapore.

(8) Bloom, J. D., Labthavikul, S. T., Otey, C. R., and Arnold, F. H. (2006) Protein stability promotes evolvability. *Proc. Natl. Acad. Sci. U. S. A. 103*, 5869−5874.

(9) Romero, P. A., and Arnold, F. H. (2009) Exploring protein fitness landscapes by directed evolution. *Nat. Rev. Mol. Cell Biol. 10*, 866−876.

(10) Weinreich, D. M., Delaney, N. F., DePristo, M. A., and Hartl, D. L. (2006) Darwinian evolution can follow only very few mutational paths to fitter proteins. *Science 312*, 111−114.

(11) DePristo, M. A., Weinreich, D. M., and Hartl, D. L. (2005) Missense meanderings in sequence space: a biophysical view of protein evolution. *Nat. Rev. Genet. 6*, 678−687.

(12) Ollis, D. L., Cheah, E., Cygler, M., Dijkstra, B. W., Frolow, F., Franken, S. M., Harel, M., Remington, S., Silman, I., Schrag, J. D., et al. (1992) The α/β hydrolase fold. *Protein Eng., Des. Sel. 5*, 197−211.

(13) Holmquist, M. (2000) Alpha/beta-hydrolase fold enzymes: structures, functions and mechanisms. *Curr. Protein Pept. Sci. 1*, 209−235.

(14) Carr, P. D., and Ollis, D. L. (2009) α/β hydrolase fold: an update. *Protein Pept. Lett. 16*, 1137−1148.

(15) Ramsden, W. (1902) Some new properties of urea. *Proc. Physiol. Soc.*, xxiii−xxvi.

(16) Tanford, C., Pain, R. H., and Otchin, N. S. (1966) Equilibrium and kinetics of the unfolding of lysozyme (muramidase) by guanidine hydrochloride. *J. Mol. Biol. 15*, 489−504.

(17) Pace, C. N. (1986) Determination and analysis of urea and guanidine hydrochloride denaturation curves. *Meth. Enzymol. 131*, 266−280.

(18) Pace, C. N. (1990) Measuring and increasing protein stability. *Trends Biotechnol. 8*, 93−98.

DOI: 10.1021/acs.biochem.5b00333
Biochemistry 2015, 54, 4330−4341

(19) Iyer, P. V., and Ananthanarayan, L. (2008) Enzyme stability and stabilization—aqueous and non-aqueous environment. *Process Biochem. 43*, 1019−1032.
(20) Eijsink, V. G. H., Bjørk, A., Gåseidnes, S., Sirevåg, R., Synstad, B., van den Burg, B., and Vriend, G. (2004) Rational engineering of enzyme stability. *J. Biotechnol. 113*, 105−120.
(21) Xie, Y., An, J., Yang, G., Wu, G., Zhang, Y., Cui, L., and Feng, Y. (2014) Enhanced enzyme kinetic stability by increasing rigidity within the active site. *J. Biol. Chem. 289*, 7994−8006.
(22) Patel, R. N. (2000) *Stereoselective Biocatalysis*, M. Dekker, New York.
(23) Bornscheuer, U. T., and Kazlauskas, R. J. (2006) *Hydrolases in Organic Synthesis. Regio- and Stereoselective Biotransformations*, 2nd ed., Wiley-VCH, Weinheim, Germany.
(24) Kourist, R., Jochens, H., Bartsch, S., Kuipers, R., Padhi, S. K., Gall, M. G., Böttcher, D., Joosten, H.-J., and Bornscheuer, U. T. (2010) The α/β-hydrolase fold 3DM database (ABHDB) as a tool for protein engineering. *ChemBioChem 11*, 1635−1643.
(25) Le, Q. A. T., Joo, J. C., Yoo, Y. J., and Kim, Y. H. (2012) Development of thermostable *Candida antarctica* lipase B through novel in silico design of disulfide bridge. *Biotechnol. Bioeng. 109*, 867−876.
(26) Martinez, C., De Geus, P., Lauwereys, M., Matthyssens, G., and Cambillau, C. (1992) *Fusarium solani* cutinase is a lipolytic enzyme with a catalytic serine accessible to solvent. *Nature 356*, 615−618.
(27) Del Vecchio, P., Graziano, G., Granata, V., Barone, G., Mandrich, L., Manco, G., and Rossi, M. (2002) Temperature-and denaturant-induced unfolding of two thermophilic esterases. *Biochemistry 41*, 1364−1371.
(28) Del Vecchio, P., Graziano, G., Granata, V., Barone, G., Mandrich, L., Rossi, M., and Manco, G. (2002) Denaturing action of urea and guanidine hydrochloride towards two thermophilic esterases. *Biochem. J. 367*, 857−863.
(29) Del Vecchio, P., Graziano, G., Granata, V., Farias, T., Barone, G., Mandrich, L., Rossi, M., and Manco, G. (2004) Denaturant-induced unfolding of the acetyl-esterase from *Escherichia coli*. *Biochemistry 43*, 14637−14643.
(30) Otzen, D. E., Giehm, L., Baptista, R. P., Kristensen, S. R., Melo, E. P., and Pedersen, S. (2007) Aggregation as the basis for complex behaviour of cutinase in different denaturants. *Biochim. Biophys. Acta, Proteins Proteomics 1774*, 323−333.
(31) Yan, G., Cheng, S., Zhao, G., Wu, S., Liu, Y., and Sun, W. (2003) A single residual replacement improves the folding and stability of recombinant cassava hydroxynitrile lyase in *E. coli*. *Biotechnol. Lett. 25*, 1041−1047.
(32) Guterl, J.-K., Andexer, J. N., Sehl, T., von Langermann, J., Frindi-Wosch, I., Rosenkranz, T., Fitter, J., Gruber, K., Kragl, U., Eggert, T., and Pohl, M. (2009) Uneven twins: Comparison of two enantiocomplementary hydroxynitrile lyases with α/β-hydrolase fold. *J. Biotechnol. 141*, 166−173.
(33) Forouhar, F., Yang, Y., Kumar, D., Chen, Y., Fridman, E., Park, S. W., Chiang, Y., Acton, T. B., Montelione, G. T., Pichersky, E., Klessig, D. F., and Tong, L. (2005) Structural and biochemical studies identify tobacco SABP2 as a methyl salicylate esterase and implicate it in plant innate immunity. *Proc. Natl. Acad. Sci. U. S. A. 102*, 1773−1778.
(34) Matthews, B. W., Nicholson, H., and Becktel, W. J. (1987) Enhanced protein thermostability from site-directed mutations that decrease the entropy of unfolding. *Proc. Natl. Acad. Sci. U. S. A. 84*, 6663−6667.
(35) Watanabe, K., and Suzuki, Y. (1998) Protein thermostabilization by proline substitutions. *J. Mol. Catal. B: Enzym. 4*, 167−180.
(36) Watanabe, K., Masuda, T., Ohashi, H., Mihara, H., and Suzuki, Y. (1994) Multiple proline substitutions cumulatively thermostabilize *Bacillus cereus* ATCC7064 oligo-1,6-glucosidase. *Eur. J. Biochem. 226*, 277−283.
(37) Sambrook, J., Fritsch, E. F., Maniatis, T. et al. (1989) *Molecular Cloning*, Cold Spring Harbor Laboratory Press, New York.
(38) Bradford, M. M. (1976) A rapid and sensitive method for the quantitation of microgram quantities of protein utilizing the principle of protein-dye binding. *Anal. Biochem. 72*, 248−254.
(39) Förster, S., Roos, J., Effenberger, F., Wajant, H., and Sprauer, A. (1996) The first recombinant hydroxynitrile lyase and its application in the synthesis of (S)-cyanohydrins. *Angew. Chem., Int. Ed. Engl. 35*, 437−439.
(40) Larkin, M. A., Blackshields, G., Brown, N. P., Chenna, R., McGettigan, P. A., McWilliam, H., Valentin, F., Wallace, I. M., Wilm, A., Lopez, R., Thompson, J. D., Gibson, T. J., and Higgins, D. G. (2007) Clustal W and Clustal X version 2.0. *Bioinformatics 23*, 2947−2948.
(41) Georgescu, R., Bandara, G., and Sun, L. (2003) Saturation mutagenesis. *Methods Mol. Biol. 231*, 75−83.
(42) Pace, C. N., and Scholtz, J. M. (1997) Measuring the conformational stability of a protein, in *Protein Structure: A Practical Approach*, 2nd ed., Creighton, T. E., Ed., pp 299−321. Oxford Univ Press, Oxford, U.K.
(43) Bushmarina, N. A., Kuznetsova, I. M., Biktashev, A. G., Turoverov, K. K., and Uversky, V. N. (2001) Partially folded conformations in the folding pathway of bovine carbonic anhydrase II: a fluorescence spectroscopic analysis. *ChemBioChem 2*, 813−821.
(44) Permyakov, E. A., Yarmolenko, V. V., Emelyanenko, V. I., Burstein, E. A., Closset, J., and Gerday, C. (1980) Fluorescence studies of the calcium binding to whiting (*Gadus merlangus*) parvalbumin. *Eur. J. Biochem. 109*, 307−315.
(45) Georlette, D., Blaise, V., Dohmen, C., Bouillenne, F., Damien, B., Depiereux, E., Gerday, C., Uversky, V. N., and Feller, G. (2003) Cofactor binding modulates the conformational stabilities and unfolding patterns of NAD^+-dependent DNA ligases from *Escherichia coli* and *Thermus scotoductus*. *J. Biol. Chem. 278*, 49945−49953.
(46) Ahmad, A., Millett, I. S., Doniach, S., Uversky, V. N., and Fink, A. L. (2004) Stimulation of insulin fibrillation by urea-induced intermediates. *J. Biol. Chem. 279*, 14999−15013.
(47) Estrada, J., Bernadó, P., Blackledge, M., and Sancho, J. (2009) ProtSA: a web application for calculating sequence specific protein solvent accessibilities in the unfolded ensemble. *BMC Bioinf. 10*, 104.
(48) Myers, J. K., Nick Pace, C., and Martin Scholtz, J. (1995) Denaturant m values and heat capacity changes: Relation to changes in accessible surface areas of protein unfolding. *Protein Sci. 4*, 2138−2148.
(49) Kemmer, G., and Keller, S. (2010) Nonlinear least-squares data fitting in Excel spreadsheets. *Nat. Protoc. 5*, 267−281.
(50) Guerois, R., Nielsen, J. E., and Serrano, L. (2002) Predicting changes in the stability of proteins and protein complexes: a study of more than 1000 mutations. *J. Mol. Biol. 320*, 369−387.
(51) Phillips, J. C., Braun, R., Wang, W., Gumbart, J., Tajkhorshid, E., Villa, E., Chipot, C., Skeel, R. D., Kalé, L., and Schulten, K. (2005) Scalable molecular dynamics with NAMD. *J. Comput. Chem. 26*, 1781−1802.
(52) Humphrey, W., Dalke, A., and Schulten, K. (1996) VMD: visual molecular dynamics. *J. Mol. Graphics 14*, 33−38.
(53) Pikkemaat, M. G., Linssen, A. B. M., Berendsen, H. J. C., and Janssen, D. B. (2002) Molecular dynamics simulations as a tool for improving protein stability. *Protein Eng., Des. Sel. 15*, 185−192.
(54) Badieyan, S., Bevan, D. R., and Zhang, C. (2012) Study and design of stability in GH5 cellulases. *Biotechnol. Bioeng. 109*, 31−44.
(55) Lakowicz, J. R. (2006) *Principles of Fluorescence Spectroscopy*, 3rd ed., Chp. 16 Protein Fluorescence, pp 529−575, Springer, New York.
(56) Huyghues-Despointes, B. M. P., Scholtz, J. M., and Pace, C. N. (1999) Protein conformational stabilities can be determined from hydrogen exchange rates. *Nat. Struct. Biol. 6*, 910−912.
(57) Padmanabhan, S., Jiménez, M. A., González, C., Sanz, J. M., Giménez-Gallego, G., and Rico, M. (1997) Three-dimensional solution structure and stability of phage 434 Cro protein. *Biochemistry 36*, 6424−6436.
(58) Vugmeyster, L., Kuhlman, B., and Raleigh, D. P. (1998) Amide proton exchange measurements as a probe of the stability and dynamics of the N-terminal domain of the ribosomal protein L9: Comparison with the intact protein. *Protein Sci. 7*, 1994−1997.

DOI: 10.1021/acs.biochem.5b00333
Biochemistry 2015, 54, 4330−4341

(59) Mayne, L., and Englander, S. W. (2000) Two-state vs. multistate protein unfolding studied by optical melting and hydrogen exchange. *Protein Sci. 9*, 1873−1877.
(60) Reetz, M. T., Carballeira, J. D., and Vogel, A. (2006) Iterative saturation mutagenesis on the basis of B factors as a strategy for increasing protein thermostability. *Angew. Chem., Int. Ed. 45*, 7745−7751.
(61) Jochens, H., Aerts, D., and Bornscheuer, U. T. (2010) Thermostabilization of an esterase by alignment-guided focussed directed evolution. *Protein Eng., Des. Sel. 23*, 903−909.
(62) Schulman, B. A., Kim, P. S., Dobson, C. M., and Redfield, C. (1997) A residue-specific NMR view of the non-cooperative unfolding of a molten globule. *Nat. Struct. Biol. 4*, 630−634.
(63) Fu, H., Grimsley, G. R., Razvi, A., Scholtz, J. M., and Pace, C. N. (2009) Increasing protein stability by improving beta-turns. *Proteins: Struct., Funct., Genet. 77*, 491−498.
(64) Hutchinson, E. G., and Thornton, J. M. (1996) PROMOTIF–a program to identify and analyze structural motifs in proteins. *Protein Sci. 5*, 212−220.
(65) Prajapati, R. S., Das, M., Sreeramulu, S., Sirajuddin, M., Srinivasan, S., Krishnamurthy, V., Ranjani, R., Ramakrishnan, C., and Varadarajan, R. (2007) Thermodynamic effects of proline introduction on protein stability. *Proteins: Struct., Funct., Genet. 66*, 480−491.
(66) Bava, K. A., Gromiha, M. M., Uedaira, H., Kitajima, K., and Sarai, A. (2004) ProTherm, version 4.0: thermodynamic database for proteins and mutants. *Nucleic Acids Res. 32*, D120−D121.
(67) Takano, K., Higashi, R., Okada, J., Mukaiyama, A., Tadokoro, T., Koga, Y., and Kanaya, S. (2009) Proline effect on the thermostability and slow unfolding of a hyperthermophilic protein. *J. Biochem. 145*, 79−85.

DOI: 10.1021/acs.biochem.5b00333
Biochemistry 2015, 54, 4330−4341